Fuzzy Control of a Gyroscopic Inverted Pendulum

F. Chetouane, *Member, IAENG,* S. Darenfed, and P. K. Singh

Abstract— **In this paper we present the efficient control imparted to an inverted gyroscopic pendulum (GIP) and demonstrate how the control mechanism through a flywheel mounted at the top of the GIP governed by a fuzzy logic controller (FLC) achieves good stability and control performance of the system around vertical position. The intuitive knowledge of controlling the GIP via a wheel momentum is fuzzified in an FLC with a base of 49 rules. FLC design is conducted using simulation before testing on real GIP plant. Compared to a proportional-integral-derivative (PID) controller it is concluded that the FLC is more suitable for stabilizing the GIP system which has a weak restoring torque.**

Index Terms— **fuzzy control, Mamdani FLC, Sugeno FLC, gyroscopic pendulum, real time control.**

I. Introduction

Development of control techniques for inverted pendulum (IP) has always remained an interesting topic to control engineers for decades. This is largely due to its physical simplicity along with complete instability. Also these control techniques are applicable to control of rockets, robots, fast moving ground vehicles and anti-seismic controls for buildings. The control goal aims at keeping the IP at an upright position, despite the natural tendency of IP to fall on either side. There are various types of IPs discussed academically followed by many kinds of control methods, e.g. Proportional-Integral-Derivative (PID), Fuzzy Logic (FL), Linear-Quadratic-Gaussian (LQG), Genetic Algorithms (GA) and Artificial Neural Networks (ANN), or any combination of these techniques. Most of the pendulums developed so far have restoring force(s) applied somehow at the fulcrum. Various linearization techniques can be used to account for nonlinearities, such as linear compensators based on Jacobian linearization. Similarly, approximate linearization was used effectively to design a controller for an inverted pendulum [1]. Some authors have considered an alternative control action consisting of an oscillatory vertical force applied to the pendulum pivot [2], [3]. The stabilizing effect of a fast vertical oscillation applied to the pendulum base is known from the early work of Stephenson [4]. Another control alternative is based on the application of a rotational torque to the pendulum base, as proposed in [5]. A hybrid LQG-Neural Controller has been studied in [6]. IPs with higher degrees of freedom are the plant of choice for control of MIMO systems [7], [8], [9], [10]. Recently a neural network control was performed on the GIP system using Nonlinear AutoRegressive Moving Average (NARMA) technique [11].

Humans manage to balance the pendulums intuitively, by applying actuation at the fulcrum, and their complicated counterparts. Although, in our case, applying a gyroscopic motion based actuation at the top of the GIP pendulum is a novel idea. This is how most biped creatures walk and balance in everyday life, or when a person spreads their arms and rotates them rapidly to restore balance and keep from falling. There is always a process of learning various techniques based on previous goals set to balance the pendulum in a vertical position. In the presented case, the GIP's fulcrum is kept in a groove so that it is only free to move on either side [12]. The restoring torque is applied through a DC motor-flywheel fixed at the top. It is a freestanding pendulum where it is swung around the fulcrum to achieve stability (see Figure 1). The GIP has much less actuating power making it *a* weak system [13]. The restoring torque depends on the gyroscopic movement of the flywheel, and the DC motor has to be run in a Min-Max voltage limit (±10 V). The GIP is a novel and a challenging plant for the design and testing of several control synthesis techniques.

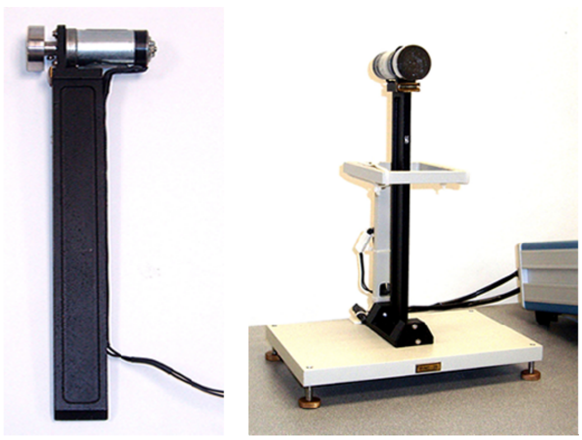

Fig. 1. The GIP is a free standing pendulum. The fulcrum is a V-shaped groove at the base allowing one degree of freedom. No bearings are used.

Manuscript received October 21, 2008. This work was supported by the National Sciences and Engineering Research Council of Canada under Grant 249484-02.

F. Chetouane is with the Electrical and Industrial Engineering Department, Université de Moncton, NB, E1A3E9 Canada (phone: 506-863-2074; fax: 506-858-4082; e-mail: chetouf@ umoncton.ca).

S. Darenfed is with the Mechanical Engineering Department, Université de Moncton, NB, E1A3E9 Canada (e-mail: darenfs@ umoncton.ca).

P. K. Singh graduated in Electrical Engineering from the Indian Institute of Technology, Kharagpur, 721302, India (e-mail: prabhatkr@gmail.com).

(Advance online publication: 1 February 2010)

In modeling a DC motor connected to a load via a shaft, the general approach is to neglect the nonlinear effects and build a linear transfer function representation for the input–output relationship of the DC motor and the load it drives. This assumption is satisfactorily accurate as far as conventional control problems are concerned. However, when the DC motor driven flywheel operates at various speeds and rotates in two directions, the assumption that the nonlinear effects on the system are negligible resulted in poor control performance for the GIP. Indeed, efforts to use a transfer function based approach to design a classical PID controller resulted in poor stability. A great advantage of fuzzy control is that nonlinear and linear systems are equally treated. To account for the nonlinearity in the system, membership functions can be customized to bring the system to a more linear behavior. The remainder of this paper is organized as follow: in the next section the dynamical model of GIP is explained. In section III, a PID controller for the GIP plant is designed using simulation. In section IV, several FLCs are designed using two different fuzzification methods: Mamdani type [14] and Sugeno type [15]. For each FLC type triangular and Gaussian membership functions are tested. Simulation is used to test-compare designed FLCs with the PID. Experimental tests with the IPNC plant and established results are discussed in section V, followed by concluding remarks.

II. GIP Dynamical Model

The GIP system has a motor and flywheel mounted atop the body (see Figure 2). Assuming such a mechanism is present in zero gravity, if the flywheel is made to rotate in the clockwise direction, the beam will rotate in the opposite direction so that the angular momentum about center of gravity of the whole assembly is conserved. Now assume that the flywheel increases its angular velocity. Hence the angular velocity of beam around the center of gravity increases (i.e. an angular acceleration is produced).

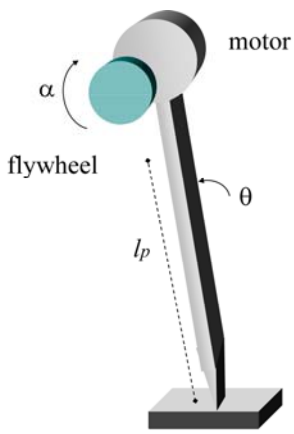

Fig. 2. GIP physical parameters.

The physical parameters of the pendulum assembly are:

m_p : mass of pendulum assembly
J_p : pendulum's moment of inertia around fulcrum
l_p : effective length of GIP (fulcrum to centre of gravity)
J_f : moment of inertia of flywheel and motor's rotor
R : motor's electrical resistance
L : motor's inductance
K : motor's torque constant
b : motor's friction factor
θ : pendulum's angular position from the vertical
α : flywheel's angular position
i : motor's armature current
V : motor's drive voltage
T_f : flywheel's generated torque
T_g : gravitational torque acting on pendulum's center
g : acceleration due to gravity

$$L \cdot \frac{di}{dt} + R \cdot i = V - K \cdot \left(\frac{d\alpha}{dt} - \frac{d\theta}{dt} \right) \tag{1}$$

$$T_f = J_f \cdot \frac{d^2\alpha}{dt^2} \tag{2}$$

$$J_f \cdot \frac{d^2\alpha}{dt^2} = K.i - b \cdot \frac{d\alpha}{dt} \tag{3}$$

$$T_g = m_p \cdot g \cdot l_p \cdot \sin(\theta) \tag{4}$$

$$T_g - T_f = J_p \cdot \frac{d^2\theta}{dt^2} \tag{5}$$

Equations (1) to (3) describe the motor-flywheel part of the system. Equation (4) describes the non-linear gravitational torque that tends to destabilize the GIP system (gravitational pull). Equation (5) describes the net torque that governs the pendulum movement around the furculum. In the next sections a PID controller and a Fuzzy Logic controller FLC are designed and evaluated for the GIP control using the non-linear GIP model and simulation with Simulink™, Mathworks Inc.

III. Design of Linear PID Controller

Figure 3 shows an overview of the control model built in Simulink™ to test the PID controller at hand and the designed FLC under several input. The PID controller model matches the analog PID supplied with the plant by the manufacturer. The PID controller ensures stabilization using set-point adaptation technique. This consists of integrating the error value (difference between set-point and the actual angular position of pendulum), and in using it to dynamically alter the set-point given by the user.

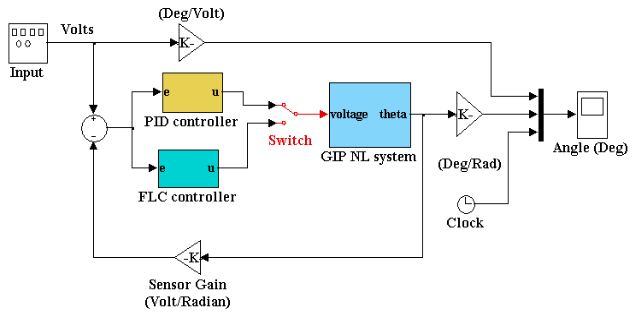

Fig. 3. GIP control model with Simulink™.

The input signal for the PID controller is fed by the position sensor measuring the deviation " θ " of GIP from the vertical, and the output signal is the control signal in volts to the motor-flywheel assembly which stabilize the GIP.

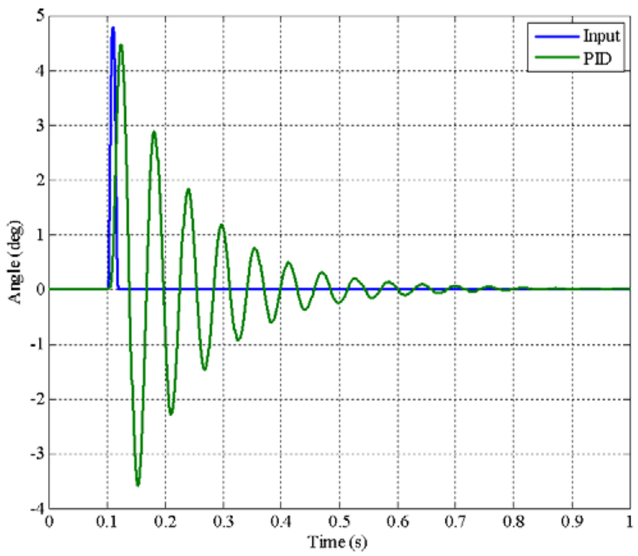

Fig. 4. Pulse response for GIP under PID control.

Figure 4 shows the GIP response with PID controller for an impulse at time 0.1 s of 5 deg. amplitude around vertical with duration of 0.01 s. The PID controller ensures stability, and fast response with a settling time *Ts*=0.59 s. While the PID performs well it requires complex tuning when applied to the real non-linear plant, here the PID parameters are P=10, I=0.5, D=0.1 and an approximate derivative factor of N=500. Thus, in the next section a fuzzy controller is designed to address the limitation of the PID controller.

IV. Fuzzy Controller Design for GIP

This section is focused on the design of a FLC for GIP system stabilisation around fulcrum. Figure 5 below shows the FLC controller model for the GIP.

Fuzzy logic is a computing approach that is based on "degrees of truth" rather than the usual "true or false" (1 or 0) Boolean logic on which modern computers are based. It was first advanced by Dr. Lotfi Zadeh of the University of California at Berkeley in the 1960. Based on the intuitive understanding of controlling the GIP with a flywheel torque several Mamdani and Sugeno types FLC are designed below. The performance of each FLC is investigated via simulation before testing on the real GIP plant. Fuzzy Inference Systems (FIS) for all FLC have two inputs: error and its derivative error rate, and one output called control.

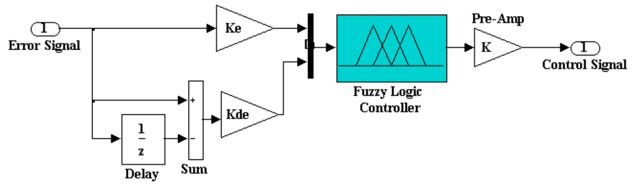

Fig. 5. GIP system FLC controller model.

The input signal error is the difference between the actual position of the pendulum and the set point (vertical position). The error signal and its derivative are conditioned using amplifier gain *Ke* and *Kde* respectively. The output variable control needs to be limited between +/- 10 V (MultiQ PCI I/O board hardware restriction) using saturation blocks.

For an FLC with two inputs and seven linguistic values for each input, there are 7^2=49 possible rules with all combinations of the inputs. The set of linguistic values for two inputs and one output with 49 rules are negative big (NB), negative medium (NM), negative small (NS), zero (ZO), positive small (PS), positive medium (PM) and positive big (PB). The input fuzzy variable *error* characterizes GIP angular displacement from the vertical position while the input fuzzy variable *error rate* characterizes the DC motor rotation speed level and direction. The output can vary from 2 to 17 V. The FLC rule base (49 rules) of the GIP system is represented by Table 1, the lines are the input *error* values, the columns are the input *error rate* values, and the corresponding argument for a line and column is the output *control* value.

TABLE I
RULE BASE FOR THE GIP SYSTEM FLC CONTROLLER

		Error rate						
		NB	**NM**	**NS**	**ZO**	**PS**	**PM**	**PB**
Error	**NB**	NB	NB	NB	NB	NM	NS	ZO
	NM	NB	NB	NB	NM	NS	ZO	PS
	NS	NB	NB	NM	NS	ZO	PS	PM
	ZO	NB	NM	NS	ZO	PS	PM	PB
	PS	NM	NS	ZO	PS	PM	PB	PB
	PM	NS	ZO	PS	PM	PB	PB	PB
	PB	ZO	PS	PM	PB	PB	PB	PB

All combinations of the error and error rate inputs lead to a total of 49 possible rules.

The fuzzification stage is completed using the linguistic values to describe the inputs and output of the FLC to specify a set of rules and to quantify this knowledge on how to control the GIP plant. All membership functions have been defined using a normalised universe of discourse [-1, 1]. Different methods for fuzzy intersection (*t*-norm) and union (*s*-norm), different membership functions (triangular, Gaussian) and different fuzzy inference methods (Mamdani, Sugeno) have been investigated to explore the effectiveness of the designed FLC using simulation. In Matlab's Fuzzy Logic toolbox, aggregation refers to the methods of determining the combination of the consequents of each rule in a Mamdani fuzzy inference system in preparation for defuzzification. Implication refers to the process of shaping the fuzzy set in the consequent based on the results of the antecedent in a Mamdani-type fuzzy inference system. Two built in *t*-norm (AND) operations are supported: minimum (*MIN*) and product (PROD). Two built in *s*-norm (*OR*) operations are supported: maximum (*MAX*) and probabilistic *OR* method (*PROBOR*). The probabilistic *OR* method is calculated according to: $PROBOR(a, b) = a+b-ab$. Thus, four different FLC controllers were designed and simulated according to the 49 rules base and to the different options offered by the Matlab Fuzzy Logic toolbox. These controllers are designated by GIP-FIS-M49, GIP-FIS-M49-GMF, GIP-FIS-S49, and GIP-FIS-S49-GMF. Controller designs are detailed in the following case studies.

A. Case 1: FLC Controller GIP-FIS-M49

In this case a Mamdani type FLC is used with triangular membership functions for the inputs and output. The FLC uses *MIN* for *t*-norm operation, *MAX* for *s*-norm operation, *MAX* for aggregation, *MIN* for implication, and *CENTROID* for defuzzification. This is shown by Figures 6 and 7.

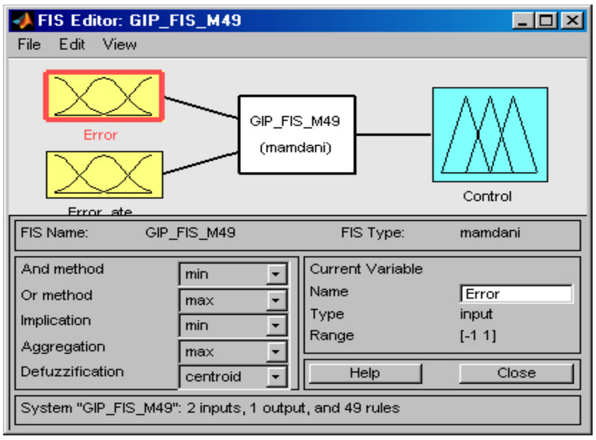

Fig. 6. GIP-FIS-M49 controller parameters.

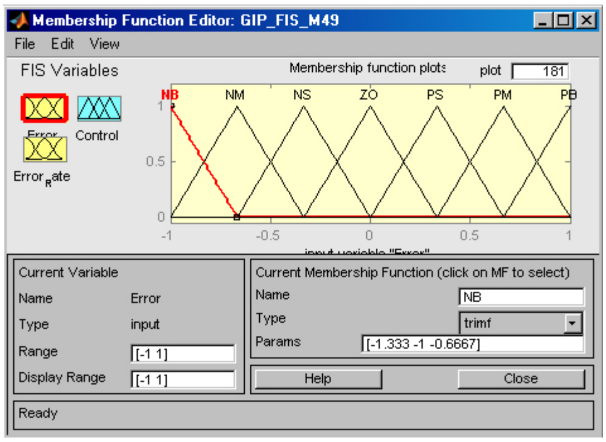

Fig. 7. GIP-FIS-M49 membership functions.

Figure 8 shows the PID controller response compared to the FLC GIP-FIS-M49 for a pulse input at time 0.1 s of 5 degree amplitude around vertical of 0.01s duration. The settling time needed by the FLC to stabilise the GIP is Ts=0.38 s compared to Ts=0.59 s with the PID controller.

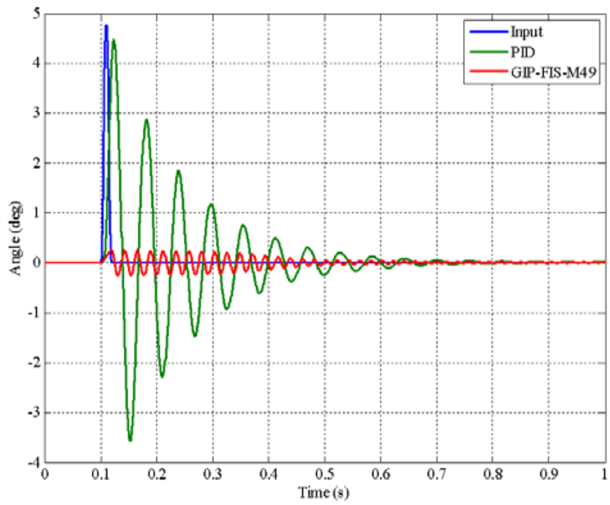

Fig. 8. GIP-FIS-M49 and PID responses.

B. Case 2: FLC Controller GIP-FIS-M49-GMF

In this case a Mamdani type FLC is used with Gaussian membership functions for both inputs and output. The FLC uses *PROD* for *t*-norm operation, *PROBOR* for *s*-norm operation, *MAX* for aggregation, *PROD* for implication and *CENTROID* for defuzzification. This is shown by Figure 9.

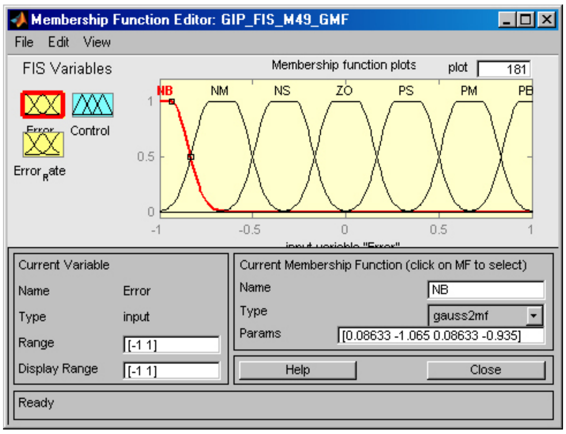

Fig. 9. GIP-FIS-M49-GMF membership functions.

Figure 10 shows the PID controller response compared to the FLC GIP-FIS-M49-GMF for the similar pulse input of 5 degree amplitude. The limit cycle response was obtained for an error derivative factor *Kde*=1 at the input of the FLC.

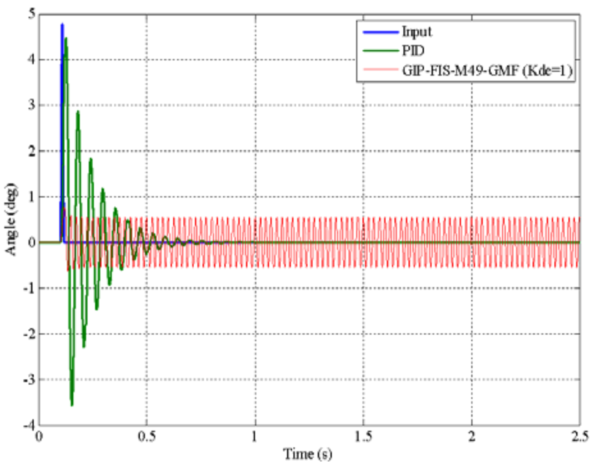

Fig.10. PID and GIP-FIS-M49-GMF (*Kde*=1) responses.

The FLC response was improved by increasing the value of *Kde* to *Kde*=5 as shown by Figure 11 where the settling time is *Ts*= 0.04 s compared to *Ts*=0.59 s with the PID controller.

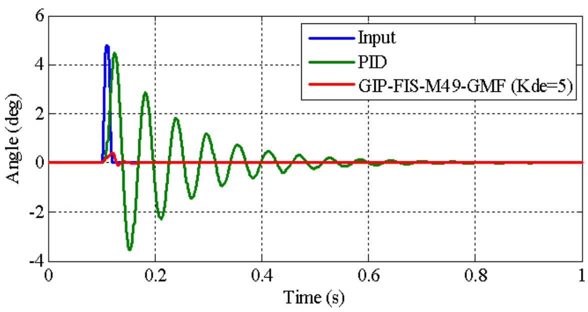

Fig.11. PID and GIP-FIS-M49-GMF (*Kde*=5) responses.

C. Case 3: FLC Controller GIP- FIS-S49

In this case a Sugeno type FLC is used with triangular membership functions for inputs and output. It uses *PROD* for *t*-norm operation, *MAX* for *s*-norm operation, and *WTAVER* for defuzzification. This is shown by Figures 12 and 13.

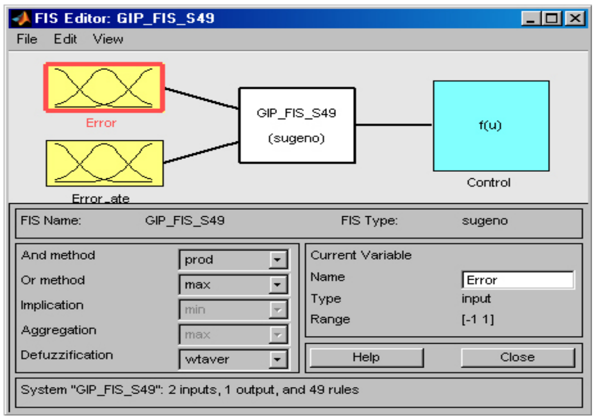

Fig. 12. GIP-FIS-S49 controller parameters.

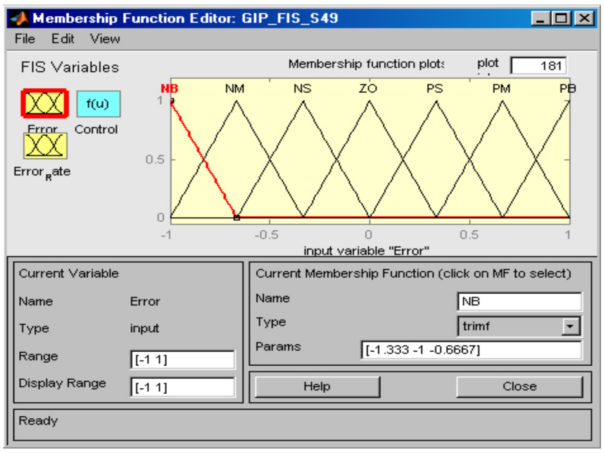

Fig. 13. GIP-FIS-S49 triangular membership functions.

Figure 14 shows the PID controller response compared to the FLC GIP-FIS-S49 for the same pulse input. The settling time needed by the FLC to stabilise the GIP is *Ts*=0.49 s compared to *Ts*=0.59 s with the PID controller.

D. Case 4: FLC Controller GIP-FIS-S49-GMF

In this case a Sugeno type FLC is used with Gaussian membership functions for both inputs and output. The FLC uses *PROD* for *t*-norm operation, *MAX* for *s*-norm operation, and *WTAVER* for defuzzification. See Figure 15.

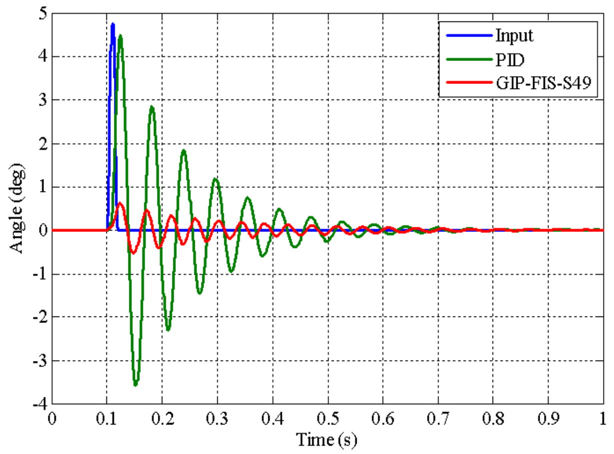

Fig.14. GIP-FIS-S49 and PID responses.

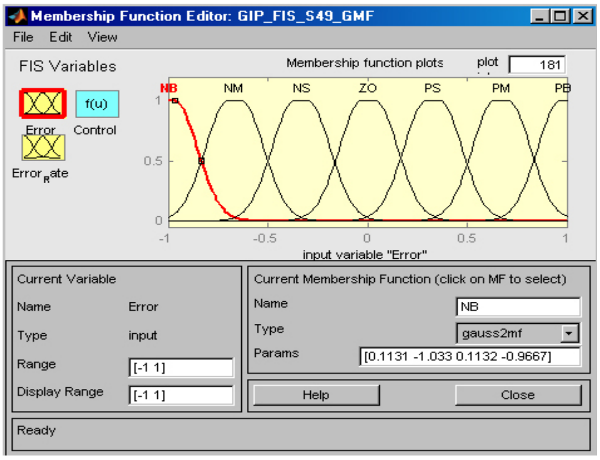

Fig. 15. GIP-FIS-S49-GMF membership functions.

Figures 16 and 17 show GIP responses under PID and GIP-FIS-S49-GMF control, for a similar pulse input of 5 degree amplitude. The value of *Ts* obtained for an error derivative factor *Kde*=1 is 1.475 s, and 0.065 s for *Kde*=5. Compared with the GIP-FIS-M49-GMF controller, the GIP response, in this case, was stable for both values of *Kde*.

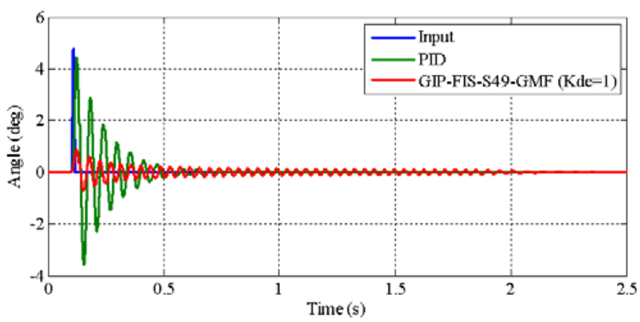

Fig. 16. PID and GIP-FIS-S49-GMF (*Kde*=1) responses.

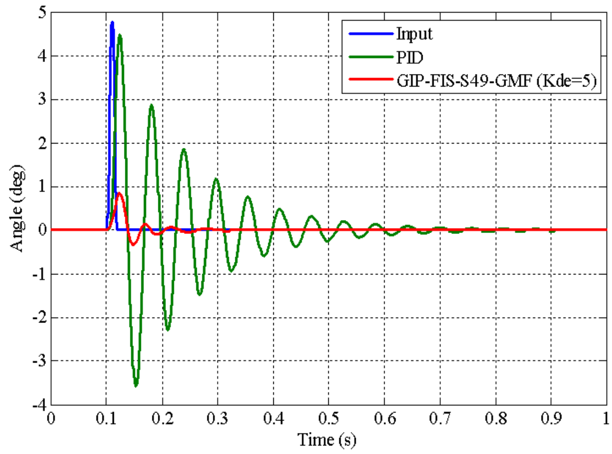

Fig. 17. PID and GIP-FIS-S49-GMF (*Kde*=5) responses.

Among the four investigated design cases it is found that FLC with Gaussian membership functions give the best simulation results. The output response was further improved by adjusting the error rate factor *Kde* for both Mamadani and Sugeno FLC types.

Tuning *Kde* allows adjusting the universe of discourses for the input membership functions and provides a GIP response with a faster settling time *Ts*. Tuning *Kde* factor was not necessary for FLC with triangular membership functions: GIP-FIS-M49 and GIP-FIS-S49. These FLCs lead to a good GIP response compared to the PID controller.

The GIP model was submitted to an additional test of tracking a square wave of 0.1 degree around vertical with a 0.5 Hz frequency. Figure 18 and Figure 19 give the FLC GIP-FIS-M49-GMF and GIP-FIS-S49-GMF responses in comparison with the PID controller. Both FLCs display a good tracking performance compared to the PID.

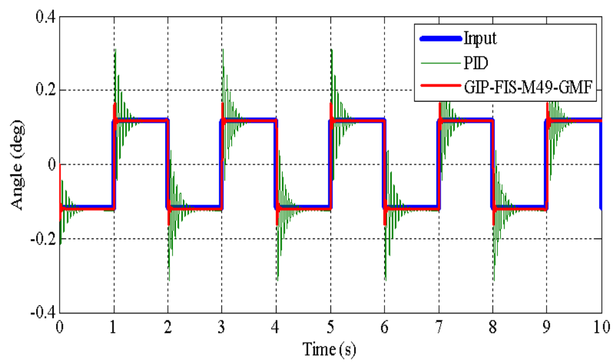

Fig.18. Tracking with GIP-FIS-M49-GMF (*Kde*=5) and PID controllers.

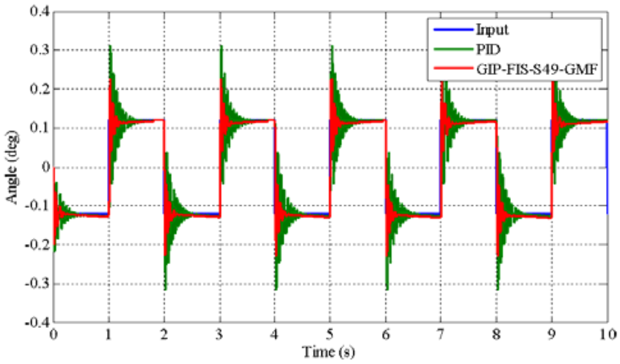

Fig. 19. Tracking test for GIP-FIS-S49-GMF (*Kde*=5) and PID controllers.

In the next section, the designed digital PID and FLCs will be applied to the control of a GIP plant called the Inverted Pendulum New Class IPNC [12].

V. Application to IPNC Real Time Control

The IPNC comes with its analog PID controller (see Figure 20). The analog PID is shutdown during these tests. Thus, the digital PID and FLCs built in Simulink™ are compiled to generate a real time control code using Wincon™ 5 software. The IPNC plant is connected as hardware in the loop with the computer to these controllers by using Quanser™ MultiQ PCI card and I/O board.

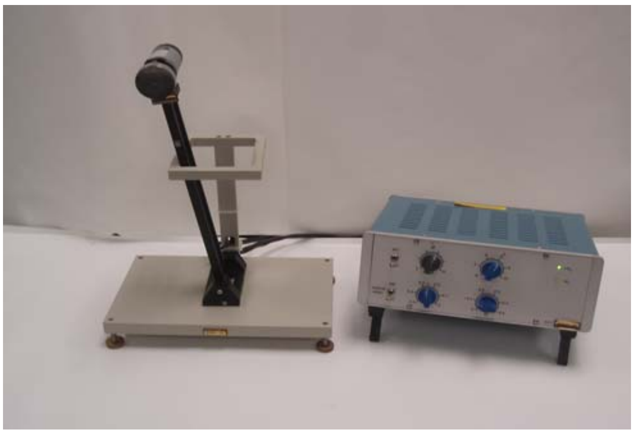

Fig. 20. The IPNC connected to an analog controller. The analog controller has a built-in PID controller. It also allows connecting external controllers and overriding its PID via an external channel.

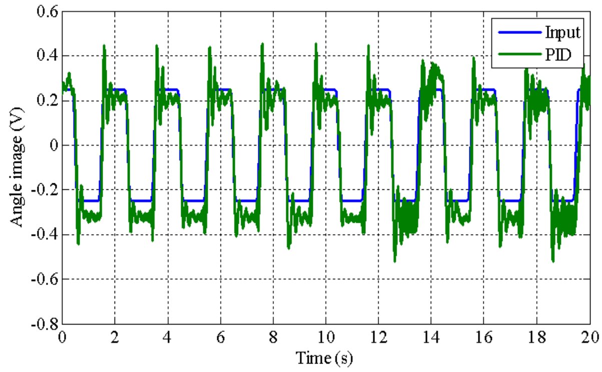

Fig. 21. Real time tracking test with the digital PID.

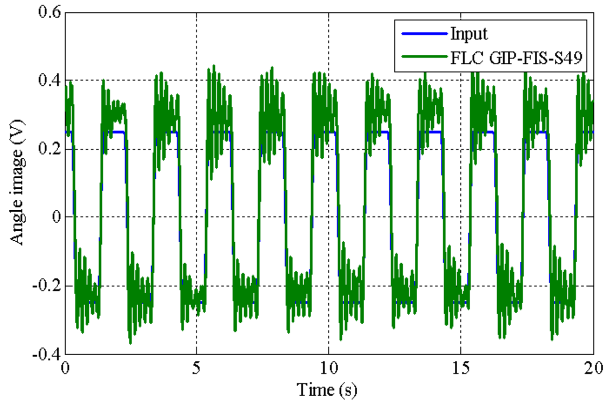

Fig.22. Real time tracking test with the FLC GIP-FIS-S49.

Figure 21 and Figure 22 show the output behavior of the IPNC under the digital PID, and the GIP-FIS-S49 controller respectively. The electrical image of the angular position is provided by the infrared sensor mounted at the GIP base.

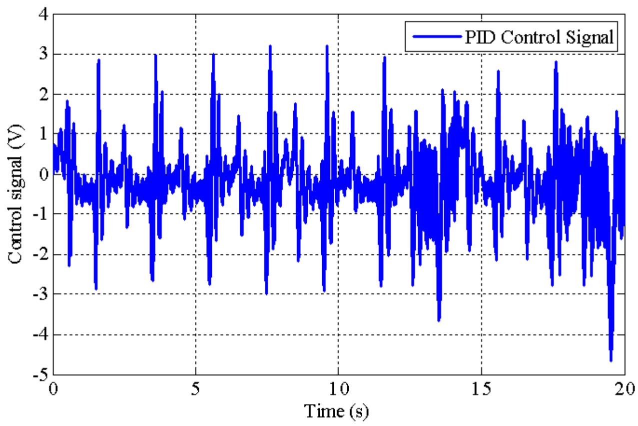

Fig.23. Digital PID control signal to the IPNC.

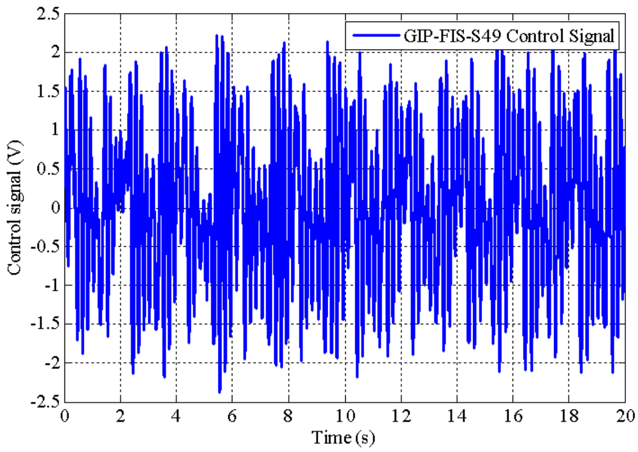

Fig.24. GIP-FIS-S49 control signal to the IPNC.

We observe good control action, as expected, and stability was satisfied by both controllers. The IPNC under digital PID controller displays fewer oscillations compared to the GIP-FIS-S49 controller. This can be caused by delays due to the computing time required by the FLC in real time.

Figures 23 and 24 show the control signal generated by the PID and the FLC. The FLC shows a better voltage delivery to the DC motor and the supplied voltage is denser and of lower amplitude. A denser control signal stabilise better the IPNC system by providing quicker restoring flywheel momentum around fulcrum. The digital fuzzy controller performance is better than the analog PID in term of power delivery to the DC motor and vibration sensed on the GIP rode.

VI. Concluding Remarks

The GIP plant introduces a novel way of balancing an inverted pendulum by the gyroscopic action of a flywheel. PD-like FLCs with two inputs, error signal and error signal derivative were designed for stabilising the GIP system. A rule set of 49 rules was formulated for each FLC controller. The FLC inputs are fuzzified in linguistic terms designed based on the expertise gained from several interactions with the IPNC GIP plant. Comparison studies of the FLC performances with two different inference methods, two different membership functions, different *t*-norm and *s*-norm operations, and different defuzzification methods have been investigated via simulation before real time control experiments. Simulation results show that all designed FLCs lead to good system performances. Among all investigated cases, it is found that FLC with Gaussian membership function provides the best simulation results (case 2, and case 4). The output response can further be improved (faster settling time *Ts*) by adjusting the *error rate* factor *Kde*, which will adjust the universe of discourses for the input and output membership functions. Real time control tests of the FLC controller were successful in stabilising the IPNC GIP. The FLC shows a better voltage delivery and less oscillation around GIP stable position compared to the PID. The Sugeno type fuzzy controller with Gaussian membership functions (case 2, with *Kde*=5) gives the best performance for real time GIP control. Further improvements will be made by designing a trainable fuzzy controller which adjusts its membership functions according to the GIP motion. This study is intended to constitute a basis for the ongoing research on intelligent control of mechanical systems using nonlinear approaches.

References

[1] T. Sugie, and K. Fujimoto, "Controller design for an inverted pendulum based on approximate linearization," *Int. J. of robust and nonlinear control*, vol. 8, no 7, pp. 585-597, 1998.

[2] P.L. Kapitsa, "Dynamical stability of a pendulum with an oscillating suspension point," *Zh. Eksp. Teor. Fiz.*, vol. 24, # 5, pp. 588-597, 1951.

[3] D. Maravall, C. Zhou, and J. Alonso, "Hybrid fuzzy control of the inverted pendulum via vertical forces," *International Journal of Intelligent Systems*, vol.20, no 2, pp. 195-211, 2005.

[4] A. Stephenson, "On a new type of dynamical stability," *Mem. Proc. Manch. Lit. Phil. Soc.*, vol. 52, no 8, pp. 1-10, 1908.

[5] I. Fantoni, and R. Lozani, "Nonlinear control for underactuated mechanical systems," *Appl. Mech. Rev.*, vol. 55, # 4, pp. 67-68, 2002.

[6] E.S. Saznov, P. Klinkhachorn, and R.L. Klein, "Hybrid LQG-Neural controller for inverted pendulum system," in *2003 Proc. 35th Southeastern Symposium on System Theory*, Morgantown, WV, 2003.

[7] A. Asgarie-Raad, "Intelligent control of two dimensional inverted pendulum," M.S. thesis, Sharif University of Technology, Iran, 1998.

[8] M. Esmailie-Khatier, "Construction and control of a two-dimensional inverted pendulum," M.S. thesis, Sharif University of Technology, Iran, 1994.

[9] A. Ghanbarie, "Neuro-fuzzy control of two dimensional inverted pendulums," M.S. thesis, Iran University of Science and Technology, Iran, 2000.

[10] P.J. Larcombe, "On the control of a two-dimensional multi-link inverted pendulum: the form of the dynamic equations from choice of co-ordinate system," *Int. J. Syst. Sci.*, vol. 23, no 12, pp. 2265-2289, 1992.

[11] F. Chetouane, and S. Darenfed, "Neural network NARMA control of a gyroscopic inverted pendulum," *Engineering Letters*, vol.16, no 3, pp. 274-279, 2008.

[12] Extra Dimension Technologies (http://www.xdtech.com), Inverted Pendulum New Class: operating manual, 2001.

[13] A. Shiriaev, A. Pogoromsky, H. Ludvigsen, and O. Egeland, "On global properties of passivity-based control of an inverted pendulum," *International Journal of Robust and Nonlinear Control*, vol.10, pp. 283-300, 2000.

[14] L.X. Wang, and J.M. Mendel, "Fuzzy basis functions, universal approximation, and orthogonal least-squares learning," *IEEE Transaction on Neural Networks*, vol.3, no 5, pp. 807-814, 1992.

[15] T. Takagi, and M. Sugeno, "Fuzzy identification of systems and its applications to modeling and control," *IEEE trans. on systems, man, and cybernetics*, vol. 15, no 1, pp. 116-132, 1985.